

Conference on scanning electron microscopy
Dearborn, MI (USA) 17-22 Apr 1983
CEA-CONF--6924

CONTRIBUTION OF SCANNING AUGER MICROSCOPY
TO ELECTRON BEAM DAMAGE STUDY

J.M. Fontaine

Service Chimie - C.E.A.-B.3

B.P. 561 - 92542 MONTROUGE CEDEX

ABSTRACT

Electron bombardment can produce surface modifications of the analysed sample. The electron beam effects on solid surfaces which have been discussed in the published literature can be classified into the following four categories : (1) heating and its consequent effects, (2) charge accumulation in insulators and its consequent effects, (3) electron stimulated adsorption (ESA), and (4) electron stimulated desorption and/or decomposition (ESD). In order to understand the physico-chemical processes which take place under electron irradiation in an Al-O system, we have carried out experiments in which, effects, such as heating, charging and gas contamination, were absent. Our results point out the role of an enhanced surface diffusion of oxygen during electron bombardment of an Al (111) sample. The importance of this phenomenon and the contribution of near-elastic scattering of the primary electrons (5 keV) to the increase of the oxidation degree observed on Al (111) are discussed, compared to the generally studied effects.

LIBRARY
19 APR 1980
U.S. ARMY

Introduction

The basic principle of Auger electron spectrometers is the electron-electron interaction. Auger spectrometers commonly use primary electron beam with energies ranging from one to a few tens of keV and currents between 10^{-9} A and 10^{-5} A. Most of them are built to provide surface analysis at high spatial resolution and therefore use highly focused electron beams ($\phi < 1000 \text{ \AA}$).

Electron-electron interactions can cause changes of the bombarded sample. The nature of these changes essentially depends on working conditions such as primary energy, composition and pressure of the residual vacuum, and sample factors like physical properties, chemical composition and morphology. The magnitude of these changes is directly dependent on the dose (Coulomb cm^{-2}) admitted in the bombarded area. The dose is defined as the product of I_p (primary current) and t (bombardment time) per surface unit. High spatial resolution Auger electron spectroscopy leads to the use of high current densities and doses and, hence, makes essential to take into account electron beam damage.

Over the last two decades, electron beam effects in Auger electron spectroscopy (AES) and scanning Auger microscopy (SAM) have been the aim of a considerable literature.

Nevertheless, there is not, to date, any systematic study of the effects because of the great number of factors on which they depend.

However, the study of the available literature dealing with this subject gives informations about the different possible kinds of beam effects which can occur in A.E.S. and S.A.M..

The first part of this paper is a brief review of the most studied effects. In AES, they may originate from several different processes.

(i) heating of the bombarded area : according to the primary energy, heating is limited to the surface or is spread into the bulk of the sample. Annealing, enhanced segregation and/or diffusion, chemical reaction etc can take place in the heated volume.

(ii) charge accumulation in non conductors : this phenomenon may give rise to field enhanced diffusion of ionic species.

(iii) electron enhanced adsorption and/or reaction (ESA) : electronic excitations of adsorbed molecules or atoms may originate excited species which reactivity towards the surface is greater than those of initially adsorbed species.

(iv) electron enhanced desorption and/or decomposition (ESD) electronic excitations of surface atoms or molecules can lead to dissociation and desorption of neutral and ionic species. The spreading of this phenomenon to bulk atoms can give rise to the decomposition of the bombarded sample.

The investigator must be acquainted with all these mechanisms. Nevertheless he must be aware that each beam effect he will experiment, is a peculiar one and hence, needs a special study.

In the second part, we report a study of the electron beam (5 keV) effects observed on Al after oxygen exposure (1000 L). The choice of proper experimental set-ups and parameters permits us to avoid or to reduce some of the above mentioned effects. The effects were observed with AES and secondary electron image (SEI). Experiments were performed both on a (111) textured polycrystalline surface and on a (100) single crystal surface, in order to check the influence of the sample structure upon the observed phenomena. We used a low current density ($9 \times 10^{-5} \text{ A.cm}^{-2}$) to avoid changing and heating effects. Experiments were repeated at different vacuum levels with different residual gas compositions in order to clear up the role of gas contamination and ESA. We explain the physico-chemical mechanism induced by the electron beam by founding upon the differences observed on the two studied surfaces. We suggest a mechanism based on the oxygen chemisorption/oxidation transition and on the electron enhanced surface diffusion of chemisorbed oxygen atoms.

Electron Beam Damages - General Considerations

Heating effect.

The electron energy loss mechanisms which take place in the scattering region can produce a local heating of the sample. This effect occurs particularly on semiconductors and insulators. Metals, with high thermal conductivities, rarely undergo heating effect.

Several approaches have been made to the calculation of the steady state temperature of surface subjected to electron bombardment (1 - 5). Baker and Sexton (5) have determined the temperature in an infinite plate (thickness L) exposed to a homogeneous electron beam (diameter $2 \cdot r_0$). In the limit $r_0 \ll L$, the maximum temperature in the spot center is given by :

$$T = \frac{P \cdot r_0}{\beta} \quad (1)$$

where β is the thermal conductivity (cal/cm.s. $^{\circ}$ C) of the plate and P the power density (Watt.cm $^{-2}$).

Vine and Einstein (1) have calculated the temperature rise $\Delta T'_0$ in the spot center, with a gaussian profile of the electronic density of the beam.

If the injected power W (Watt) is dissipated only on the surface $\Delta T'_0$ is given by :

$$\Delta T'_0 = \frac{0,099 W}{\pi^{1/2} \cdot \beta \cdot a_1} \quad (2)$$

where a_1 is the full width at half maximum of the electronic density of the beam (cm).

If the backscattering of electrons is considered, equation (2) must be corrected by a factor p; characteristic of the non-backscattered power ratio.

The temperature rise is then given by :

$$\Delta T_0 = p \cdot \frac{0,099 \cdot W}{\pi^{1/2} \cdot \beta \cdot a_1} \quad (3)$$

A model has been proposed by Archard (6) for the calculation of p .

Vine and Einstein (1) have shown that equation (3) must be corrected by a function of the ratio $\frac{x_0}{d}$, if one takes into account the penetration of primary electrons. d is the beam diameter and x_0 , the total range of primary electrons, can be calculated by the Thomson-Widdington law (1). This correction is necessary only for primary energies E_p higher than 10 keV and d below 1 μm . It may be generally neglected in A.E.S..

By using the model proposed by Vine and Einstein, we have calculated the temperature rises on Al ($\beta = 0,567 \text{ cal/cm}^\circ \text{C.s}$) and SiO_2 ($\beta = 32 \cdot 10^{-4} \text{ cal/cm}^\circ \text{C.s}$) with different bombardment conditions (Fig. 1).

Röll (7, 8) and Montmitonnet and Darque-Ceretti (9) have proposed calculations of the temperature distribution in a thin film as a function of the film thickness, taking into account that the film is deposited on a substrate of different thermal conductivity. These calculations are in good agreement with results obtained on multilayer Ni-Cu films (10) and on Au/Ag sandwich films (11) exposed to electron beam and show that the radial heat transport in irradiated metal films plays an important role.

The thermal damage is even more important when insulating materials are bombarded with electron beams. Madey et al. (12) report that insulating powders have been heated to incandescent temperatures during Auger electron analysis.

Yau et al. (101) have calculated the depth and radial distributions of temperature in a silica target bombarded with a 0,5 μm diameter electron beam ($E_p = 2 \text{ keV}$, $I_p = 1 \mu\text{A}$).

The temperature rises up to 1100°C at the surface. The depth and radial temperature gradients are very steep. It is obvious that such densities ($> 100 \text{ A.cm}^{-2}$) must be avoided on insulating materials. Therefore, low electron beam currents (10^{-9} A) must be used to perform high spatial AES on such materials.

Charging effects

The examination of insulating materials with AES is often complicated by charging of the bombarded area (13-15). This effect depends on the total secondary electron yield δ of the bombarded surface. δ depends on the primary energy E_p (16,17). Its variations are shown in Fig. 2. Adsorbed layers and sample temperature can also influence the value of δ .

On insulating materials, it is generally advised to use very low current density and to choose a primary energy which corresponds to a secondary electron yield close to unity.

Moreover, electron bombardment can give rise to an electron accumulation in the sub-surface. This effect, combined with a positive surface potential can lead to the electromigration of ionized species in the surface region. Lineweaver (18) has shown the existence of a negative charge in the sub-surface of SiO_2 bombarded with electrons. He has shown that the negative charge is located at a depth corresponding to the maximum diffusion length of incident electrons. Sasaki (19) has noted, during XPS examination of Li_2WO_4 films previously bombarded with 1 keV electrons,

that photoelectrons were accelerated by a sub-surface charge which persisted after electron bombardment.

Many workers have observed by AES the field-induced diffusion of ions (20-26) in glasses submitted to electron bombardment. Pantano et al. (24,25) have discussed the decay of the sodium Auger signal in soda-lime silicate glasses. They have shown that the mechanism responsible for the observed phenomena was field-induced migration rather than electron-stimulated desorption (ESD). This result is confirmed by microprobe analysis of glasses (27-30).

More recently, Vigouroux et al. (31) have proposed a new model on the electrical conduction phenomena in glasses. This model, based on the band diagram of glasses, should supply a general explanation to the charging phenomena observed in electron-bombarded insulators.

Electron Stimulated Adsorption (ESA)

Since AES is a surface sensitive technique, and since the surface of clean solids may be very reactive, it is necessary to perform the measurements in ultrahigh vacuum (UHV) systems (10^{-9} - 10^{-11} Torr). The sticking coefficient of residual gasses (H_2 , H_2O , CO) on clean surfaces are generally low enough to allow meaningful AES analysis with such vacuum conditions. However, many authors (32-45) have reported on electron stimulated adsorption (ESA) of gasses on electron bombarded surfaces. This effect is usually attributed to electronic excitation and/or dissociation of molecules in the gas phase close to the surface, or of molecules chemisorbed on the surface. It results an increased reactivity of these excited molecules towards the surface and an enhanced reaction, generally limited into the bombarded area.

Different mechanisms have been proposed depending on the gas/surface system which is studied. The most frequently proposed one is based on electronic excitation and dissociation of adsorbed molecules leading to stimulated reaction and/or surface and/or bulk stimulated diffusion (35-39).

However, the interpretation of ESA phenomena is often very complex.

Thus, the quite opposite results obtained by Coad et al. (32) and by Joyce and Neave (33,34) on the electron stimulated adsorption of CO on Si (111) are really surprising.

These authors have worked exactly in the same experimental conditions (Si (111) ; $E_p = 2 \text{ keV}$, $d = 10^{-4} \text{ A.cm}^{-2}$, $p_{\text{CO}} = 5.10^{-10} \text{ Torr}$). The only explanation of the opposite phenomena they observed (Coad et al. (32) got oxygen stimulated adsorption in the bombarded area whereas Joyce and Neave (33,34) observed carbon stimulated adsorption) is the difference of the impurity levels of the bombarded surfaces. Coad et al. (32) have shown that the carbon contamination increase during electron bombardment was dependent on the initial cleanness of the surface.

The understanding of ESA mechanisms needs a thorough characterization of the surface (structure, composition, impurities), the more as very low impurity levels can greatly influence the development of the studied phenomenon.

Electron stimulated desorption (ESD)

Electron stimulated desorption is a widely studied phenomenon (46-54). When slow electrons impinge on solid surface covered with adsorbate layers, desorption of ions, and/or neutrals can occur. This effect is used as a probe for investigation of adsorbate states. Unfortunately, it can also be a disturbance in other surface analysis methods which use electron bombardment as excitation source. Its mechanism depends on the electronic nature of the system surface/adsorbate and is connected with the available transitions between the different adsorbate levels.

A phenomenological model of the ESD process, based on a one-dimensional classical theory, has been proposed by Redhead (49-51) and by Menzel and Gomer (47,48). It is described in a simplified manner by the potential energy diagram drawn in Fig. 3.

It has been suggested in (47-51) that ESD process is similar to the dissociative ionization of free gas molecules except that in the ESD mechanism, the ionization of adsorbed atoms or molecules can be followed by the neutralization of the freshly formed ions in their travel away from the surface. The latter effect is responsible for the desorption of neutral atoms and for the possible recapture of the desorbing species by the surface (Fig. 3). This recapture explains the fact that ESD cross-sections are 2-3 orders of magnitude smaller than the cross-sections for the dissociative ionization of free gas molecules (e.g., for CO on tungsten, values between 10^{-17} and 10^{-21} cm² are found for different states (52)). There are other possible mechanisms which are not considered here ; for example, direct excitation into antibonding states, and direct desorption as metastable or

or excited atoms. In the case of recapture, the kinetic energy of the desorbing species is transferred to the surface as thermal energy or can be responsible for the surface diffusion of the adsorbed species after their recapture.

ESD of adsorbed layers must be thoroughly considered in AES especially for weakly bound chemisorbed species for which ESD cross-sections lie between 10^{-17} and 10^{-19} cm^2 . For more strongly bound species, cross-sections mostly lie between 10^{-19} and 10^{-21} cm^2 . The model of ESD can be extended to the desorption of impurities from a matrix. Moore (57) and Petermann (58) have shown that impurities can be removed by ESD with a yield varying between 10^{-9} to 10^{-5} per incident electron.

The decomposition under electron bombardment of ionic compounds such as metal oxides, SiO_2 and glasses, has been the aim of many investigations (13,15,18,27,28,59-70). On these materials, removal of oxygen and reduction of the bombarded surface have been clearly displayed by AES measurements. In some of these studies (13,15,59,61) the breaking of the Si-O bond has been explained in terms of an ESD mechanism based on the Redhead (49-52) Menzel and Gomer (47,48) model. More recently, Knotek and Feibelman (71,72) have proposed for ionic compounds an ESD mechanism which originates by interatomic Auger transitions. Electron impact produces a core hole on the cation. An interatomic Auger process follows which leads to a "Coulomb explosion". In this process, the anion can be converted to a cation. The electrostatic repulsion between this cation and the metal cation could explain the O^+ desorption and the consecutive reduction observed on metal oxides. Knotek and Feibelman (73) have proposed criteria for the stability

of ionically bonded compounds in ionizing environments. They provide that the materials most likely to decompose under electron bombardment are maximal valency compounds in which the cation and the anion have Pauling electronegativity differences > 1.7 . (e.g. SiO_2 , Al_2O_3 , TiO_2 , V_2O_5 , WO_3 , MoO_3 ,...). Van Oostrom (63) has studied the reduction of Al_2O_3 to Al under electron bombardment. He has shown that the onset for decomposition is near 10 Ccm^{-2} for a 5 keV electron beam.

This preferential removal process seems to apply to alkali halides, on which the desorption of halogen atoms has been observed (74-83). It is not well established whether this process is the same as for the metal oxides (80), or is due to electronic excitations and thermal effects (74-79) or involves the diffusion of defects (e.g. F centers) to the surface (81-83).

The stability of many other materials submitted to electron bombardment has been studied and the results have been related by Madey et al. (84).

The lack of a systematic study of electron beam damages originates from their wide spread. A review paper on this subject, by Pantano and Madey (85) puts forward how complex such a study could be. Moreover, such a study could not treat of each particular case, especially concerning practical or technological samples. Thus, it could be more useful for investigators to dispose of some guidelines for avoiding electron beam and, principally, a proceeding to take up the problem of electron beam damage and check up the contribution of the different processes generally involved in electron beam effects. In the second part of this paper, we present a study of the electron beam effects on an aluminum sample exposed to oxygen. In this work, the careful examination of all processes,

especially ESA and ESD, enables us to confirm the electron enhanced surface diffusion of adsorbed species (86) and to display the contribution of a direct momentum transfert mechanism to the observed phenomena.

Electron beam effects on oxygen exposed aluminium surface

In a previous experiment (87) we have shown, on an oxygen exposed (111) textured polycrystalline aluminum surface the reduction effect of a 250 eV electron beam and the oxidation effect of a 5 keV electron beam (Fig. 4). These effects are accompanied by contrast modifications of the secondary electron-image of the bombarded area : (i) darkening during reduction ($E_p = 250$ eV) and brightening during oxidation ($E_p = 5$ keV). (Fig.5)

We will report here, the results of the experiment carried out for a better understanding of these effects.

Experimental :

The experiment was performed in a JEOL JAMP 10 Scanning Auger Microscope. The system is equipped with an ion pump, a titanium sublimation pump and a cryogenic panel. The basic vacuum is 10^{-9} Torr without baking out and without using the cryogenic panel. The primary electron beam is perpendicular to the sample surface. The electron spectrometer is a cylindrical mirror analyzer (CMA) which axis is parallel to the surface. A beam brightness modulation system enables us recording the E.N (E) distribution of the emitted electrons. The first and second derivative curves can be obtained by modulating the potential of the external cylinder of the CMA. Sample cleaning is achieved with ion bombardment (Ar^+ , 10^{-6} A.cm⁻², 3 keV).

Two aluminum samples were used for this experiment :

(i) the polycrystalline sample studied in the previous experiment (87). It was of purity 99,99 %. It was mechanically polished to a mirror-like finish and then ion etched (Ar^+ , 3 keV, $10^{-6} \text{ A.cm}^{-2}$) at 450°C until the surface plasmon peak and the 4 eV loss (88-89) observed with a 250 eV primary energy were well-defined. The sample was then heated to 550°C for half an hour. After this treatment, the sample consisted of big grains (1-2 mm). It has been checked with X-Ray diffraction that all grain surfaces were (111) oriented within a few degrees.

(ii) a single crystal Al (100). It was mechanically polished and then electrochemically polished in a solution of perchloric acid and ethyl alcohol. Ion etching and heating have been performed in the same manner as for the first sample. Same cleanness criterions have been used.

In order to compare the evolution of the electron bombarded surface with that of the non bombarded surface, we have selected beforehand five spots (labelled A to E) on each sample (located on one big grain on the (111) Al sample). The evolution of the surface under electron bombardment is checked every 5 min. on the spot A, on which the electron beam is kept for more than 1 h, except during the spectra acquisition periods from the non-bombarded surface (i.e spots B to E). Preliminary measurements showed that no difference could be detected by AES ($E_p = 5 \text{ keV}$) or by ELS ($E_p = 250 \text{ eV}$) among these five spots. The sample surface was ion etched before each run of oxygen exposure and A.E.S. acquisitions.

During oxygen exposures, the valve separating the gun chamber and the main chamber was closed. For AES acquisition, energy ranges from 0 to 80 eV and from 470 to 525 eV were studied. AES acquisitions were performed with the same conditions than that used for bombardment.

Results and discussion

- AES study of the initial steps of the aluminum oxidation

Fig. 6 shows the Auger spectra of the Al (111) surface after different oxygen exposures (0 → 1000 L). The evolution of the Al (100) Auger spectra were similar. Fig. 7 shows the decrease of the peak-to-peak height of the Al_{LVV} peak (at 68 eV) (derivative mode) on the (111) surface, normalized to that of a clean surface, for exposures ranging from 0 to 50 Langmuirs. We have collected on Fig. 8 the variations of the peak to peak heights of the Al_{LVV} peaks (the peak located at 68 eV ; called in abbreviation the Al peak, characteristic of the aluminum metal and that located at 54 eV, later called the Al - O peak, characteristic of the oxidized aluminum), and the oxygen O_{KLL} peak located at 508 eV (90-92) for exposures from 0 to 1000 Langmuirs. Moreover, we have shown on the figure the variations of the ratio of Al-O peak height over the sum of the heights of the Al and Al-O peaks (defined as R). In this work we will use the value of R to represent the extent of the surface oxidation.

- Electron beam effects

On a clean Al (111) surface, no appreciable difference could be observed in A.E.S. between the bombarded area (spot A, 70 mm, 5 keV, $9 \times 10^{-5} \text{ A.cm}^{-2}$) and the non-bombarded surface (spot E) examined after the bombardment of the spot A.

We have observed on the both areas (A and E) a slight decrease of the Al_{LVV} peak and the apparition of the oxygen Auger peak. In both cases, it corresponds to a 4 - 5 Langmuirs oxygen exposure. This result seems compatible with a residual gas contamination ($2,5 \times 10^{-9}$ Torr). We got similar results on the Al (100) surface. On such clean surfaces, electron bombardment effects (5 keV , $9 \times 10^{-5} \text{ A.cm}^{-2}$, 70 mn) seem negligible compare to the vacuum contamination.

Electron beam irradiation (5 keV , $9 \times 10^{-5} \text{ A.cm}^{-2}$, 70 mn) effects were then studied on the Al (111) surface exposed to 100, 250 and 1000 L of oxygen. The same effects have been observed for the three exposures :

(i) the O_{KLL} peak height increases in the bombarded area (spot A) (Fig. 9a solid line). The increase value is about 20 % of the O_{KLL} peak height measured on the non-bombarded surface (spots B, C, D and E) (Fig.9a, dashed line).

(ii) the R value also increases in the bombarded area (Fig. 9b, solid line). The relative increase of R is the same for the different exposures : about 40 % of that measured in the non-bombarded area (Fig. 9b). It is worthy to note the slight increase of R on the non-bombarded surface (spot B C D and E) (Fig.9b dashed line).

The difference between solid lines (bombarded area) and dashed lines (non-bombarded surface) can be used to represent the effect of electron bombardment.

The SEI observation of the bombarded area shows a bright contrast. This contrast can be removed by ion etching at 500 eV for a couple of minutes, thus suggesting a very superficial beam effect.

Same experiment has been repeated on a 1000 L exposed (111) aluminum surface with different current densities (9×10^{-5} , 3×10^{-4} , $1,1 \times 10^{-3}$ and $2,3 \times 10^{-3}$ A.cm⁻²). These densities were obtained by keeping constant the primary intensity ($2,2 \times 10^{-8}$ A) and primary energy (5 keV) and varying the beam diameter (respectively 175, 100, 50 and 35 μ m). We observed that :

(i) the initial value of the O_{KLL} peak height ($t = 0$) and its increase were the same in all cases

(ii) the initial value of R ($t = 0$) increased in proportion to the current density (Fig. 10) but its final value ($t = 70$ mn) in the bombarded area (spot A) was the same whatever the density. The acquisition of the AES spectra from 0 eV to 70 eV (energy range scanned to record the Al-0 and Al peaks) took about 70 s. Thus, the higher initial R value at higher current density corresponds to the higher dose (current density \times time) accumulated in the bombarded area during 70 s.

The different behaviors of the variations of the O_{KLL} peak height and that of the R value suggest that the mechanisms responsible for these variations may be different.

The oxygen increase only depends on the primary intensity, thus indicating that this phenomenon is not restricted into the bombarded area but concern a greater part of the sample. On the other hand, the R behavior suggests that the variations of R during bombardment are the consequences of two possible successive mechanisms.

(i) the first one, with a rapid kinetic, which depends on the current density and thus on the species initially present in the bombarded area.

(ii) the second mechanism, with a slower kinetic, which is directly correlated to the oxygen increase in the bombarded area. Its kinetic is not dependent on the current density.

- Influence of the vacuum level

The increase of the oxygen concentration and of the oxidation rate under electron bombardment are often attributed to electron stimulated adsorption of the residual vacuum molecules. In order to check the vacuum contribution to the observed phenomena, electron bombardment (5 keV, 9.10^{-4} A.cm⁻², 70 mm) of the Al (111) oxygen exposed (1000 L) surface has been carried out during cooling the cryogenic panel. The liquid nitrogen cooled cryogenic panel can not only decrease the vacuum level (6.10^{-10} Torr instead of $2,5.10^{-9}$ Torr), but also changes the composition of the residual gases. The gas composition has been analysed by using quadrupole mass analyser (RIBER QS 200) : without using the cryogenic panel, the main components are H₂O and CO ; upon cooling the cryogenic panel, H₂O is readily removed.

On these vacuum conditions, electron bombardment effect (5 keV, 9×10^{-5} A.cm⁻², 70 mm) is similar to that obtained without cooling the cryogenic panel.

This result rules out the contribution of electron stimulated adsorption : removing the major source of oxygen in the chamber (H₂O) does not change the phenomenon.

This result suggests that the increase of the oxygen concentration and the increase of the oxydation rate are not due to electron beam stimulated adsorption of residual gases. It is confirmed by the absence of electron beam effect on the clean Al (111) surface.

The consequence of these results is : the source of oxygen is the sample itself. Nevertheless, two main mechanisms are available : (i) bulk diffusion of the oxide incorporated oxygen or/and (ii) surface diffusion of oxygen. The last mechanism can involve the oxygen of the aluminum oxide or/and the chemisorbed oxygen.

Electron bombardment of aluminum oxide gives rise to oxygen desorption and reduction of the bombarded surface (63). Then, we have ruled out the contribution of the aluminum oxide to the observed phenomena. This hypothesis limits the source of oxygen to the oxygen chemisorbed phase. The oxygen-aluminum interaction has been extensively investigated (93-99). It has been shown that the initial oxidation greatly depends on the surface orientation. It is generally accepted that on the (100) and (110) faces, oxygen incorporates into the bulk and gives rise to oxide formation for sub-monolayer coverage. On the (111) face, a chemisorbed oxygen layer is formed initially, which is then transformed into oxide upon further oxygen exposure. We have used this difference to confirm the hypothesis of oxygen chemisorbed surface diffusion. The single crystal Al (100) has been electron bombarded (5 keV, 9×10^{-5} A, 70 mm) after oxygen exposure (1000 L). After irradiation, the R value increased by about 5 % over that of the non irradiated surface and the oxygen concentration was the same (within noise level) in the irradiated and non irradiated areas (Fig. 11a). The absence of electron bombardment effect on the Al (100) oxygen exposed surface confirms that electron beam effects on Al (111) occur in the oxygen chemisorbed phase.

The increase of the oxygen concentration into the bombarded area is the consequence of the surface diffusion of the chemisorbed oxygen.

We think that this phenomenon takes place on the whole sample surface. It is probably enhanced by secondary electrons which are scattered by the chamber walls and principally by the objective lens of the electron microscope (Fig. 12). These low energy electrons are responsible for electronic excitations which can lead to a desorption re-capture - surface diffusion mechanism (see electron stimulated desorption). The kinetic of such a mechanism does not depend on the current density but on the primary current intensity as it is observed in our experiments. The existence of this mechanism is confirmed by the sample reduction observed under a 250 eV electron bombardment.

The opposite phenomena observed at 250 eV and 5 keV make difficult the explanation of the increase of the R value (Al (111) - 5 keV) in terms of electronic excitations.

On Al (111) the oxidation state is separated for the oxygen chemisorbed state by a potential barrier. This barrier can be overcome by heating the sample. The transition temperature was reported to be 450°C for a 30 L exposure (99) and 160-200°C for 100 L exposure (98). These temperatures correspond to an estimated activation energy of 1 eV at 0 L (98). The activation barrier height decreases with the coverage rate of the surface : after 1000 L exposure, we observed with low current density ($9 \times 10^{-5} \text{ A.cm}^{-2}$) an increase at room temperature of R, even on the non-bombarded surface (Fig. 9b, dashed line), whereas the oxygen concentration remains constant (Fig. 9a dashed line). We have estimated the average value of the activation barrier for oxygen incorporation on Al (111) exposed to 1000 L of oxygen to be about 100 meV. Then it is possible for the chemisorbed oxygen atoms to get this activation energy through quasi-elastic scattering

of the 5 keV primary electrons. We have shown the cross-section of elastic-scattering of the 5 keV primary electrons to transfer more than 100 meV to a chemisorbed oxygen atom is about $2 \times 10^{-19} \text{ cm}^2$ (100). This value emphasizes the importance of such a phenomenon : with a current density of $9 \times 10^{-5} \text{ A.cm}^{-2}$ the probability for a chemisorbed atom to be incorporated through an elastic scattering process is 0.1 in 15 minutes.

The almost high value we have found for the oxydation process cross-section explains the different initial values of R we measured with different current densities. The existence of two different processes responsible for oxygen concentration increase and oxidation extent increase explains the kinetics we have observed.

The kinetic of increase of the R value can be analysed in two parts : (i) A rapid phenomenon : incorporation of the oxygenen chemisorbed atoms located in the bombarded area ; its kinetic depends on the current density (ii) a slow phenomenon : diffusion of oxygen chemisorbed atoms of the non-bombarded surface towards the bombarded area where free adsorption sites have been created by incorporation. These new oxygen atoms can be in turn incorporated by incident electrons.

Conclusion

Electron bombardment effects in AES have been the aim of a considerable number of studies. These studies have permitted a rough classification of the observed effects in four categories : (i) thermal effects, (ii) electrical effects, (iii) electron enhanced adsorption or reaction (iv) electron enhanced desorption and decomposition. In spite of a considerable literature on this subject, no systematic study of electron beam damage in AES exists, but most of factors which can contribute to analysis error and sample damage are known and some general guidelines can be given on how to minimize electron beam effects. However, certain effects which involve physico-chemical processes are genuine and cannot be completely eliminated. We have shown that the chemisorbed - oxide transition observed on the Al (111) oxygen exposed surface is caused by near-elastic scattering of the primary electrons (5 keV) and cannot be completely eliminated even by working with very low current densities ($9 \times 10^{-5} \text{ A.cm}^{-2}$). The surface diffusion of chemisorbed oxygen we have observed is perhaps more pronounced in a microscope-spectroscope combined device but such a mechanism should be generally studied and its contribution compared to that of electron stimulated adsorption (ESA).

References

1. J. Vine and P.A. Einstein : "Heating Effects of an Electron Beam Impinging on a Solid Surface, Allowing for Penetration".
Proc. IEEE, 111, n° 5 (1964), 921-930.
2. L.G. Pittaway : "The Temperature Distribution in Thin Foil and Semi-Infinite Targets Bombarded by an Electron beam" Brit. J. Appl. Phys, 15 (1964) 967-982.
3. M. Lax : "Temperature Rise Induced by a Laser Beam"
J. Appl. Phys. 48 (1977) 3919-3924.
4. M. Lax : "Temperature Rise Induced by a Laser Beam II. The Nonlinear Case". Appl. Phys. Letters 33 (1978) 786-788.
5. B.G. Baker and B.A. Sexton, "Electron Beam Effects in Auger Analysis of Physisorbed Xenon". Surface. Sci. 52 (1975) 353-364.
6. G.D. Archard : "Back-Scattering of Electron". J. Appl. Phys., 32 (1961), 1505-1509.
7. K. Röhl : "The Temperature Distribution in a Thin Metal Film Exposed to an Electron Beam". Appl. Surf. Sci. 5 n° 4 (1980) 388-397.
8. K. Röhl, W. Losch : "Temperature Rise in Thin Films During Auger Depth Profiling". Proc. 8th Int. Vac. Congr. and 4th Int. Conf. Solid. Surfaces (1980) Cannes.

9. P. Montmitonnet and E. Darque - Ceretti : "Echauffement d'un Matériau Bicouche Soumis à un Faisceau Electronique". J. Microsc. Spectrosc. Electron., Vol. 7, 1982, 615-627.
10. K. Röhl, W. Losch and C. Achete : "Electron-Beam-Induced Diffusion During Thin Film Depth Profiling". J. Appl. Phys. 50 (1979) 4422-4424.
11. S. Hofmann and A. Zalar : "Electron Beam Effects During the Sputter Profiling of Thin Au/Ag Films Analysed by Auger Electron Spectroscopy". Thin Solid Films 56 (1979) 337-342.
12. T.E. Madey, C.D. Wagner and A. Joshi. Surface Characterization of Catalysts Using Electron Spectroscopies : Results of a Round - Robin Sponsored by ASTM Committee D.32 on Catalysts. J. Electron Spectrosc. and Rel. Phenom. 10, (1977), 359-388.
13. B. Carriere and B. Lang : "A Study of the Charging and Dissociation of SiO₂ Surfaces by AES", Surface Sci. 64 (1977) 209-223.
14. B. Lang and S. Goldsztaub, "Charging of Insulators in LEED Studies", Surface Sci. 32 (1972) 473-476.
15. S. Thomas, "Electron Irradiation Effect in the Auger Analysis of SiO₂". J. Appl. Phys. 45 (1974) 161-166.

16. A.J. Dekker "Secondary Electron Emission".
Solid State Phys. 6 (1958) 251-311.
17. O. Hachenberg and W. Brauer, "Secondary Electron Emission from Solids".
Adv. Electronics and Electron Phys. 11 (1959) 413-499.
18. J.L. Lineweaver, "Oxygen Out Gassing Caused by Electron Bombardment of Glass". J. Appl. Phys. 34 (1963) 1786-1791.
19. T. Sasaki, R.S. Williams, J.S. Wong and D.A. Shirley, "Radiation Damage Studies by X-Ray Photo Electron Spectroscopy".
I. Electron Irradiated LiNO_3 and Li_2SO_4 .
II. Electron Irradiated Li_2CrO_4 and Li_2WO_4 ,
J. Chem. Phys. 68 (1978) 2718-2724 ; 69 (1978) 4374-4380.
20. N.J. Chou, C.M. Osburn, Y.J. Van Der Meulen and R. Hammer,
"Auger Analysis of Chlorine, in "HCl or Cl_2 Grown" SiO_2 films",
Appl. Phys. Letters 22 (1973), 380-381.
21. P.T. Dawson, O.S. Heavens and A.M. Pollard, "Glass Surface Analysis by Auger Electron Spectroscopy". J. Phys. C.11 (1978) 2183-2193.
22. R.A. Chappell and C.T.H. Stoddart, "An Auger Electron Spectroscopy Study of Float Glass Surfaces". Phys. Chem. Glasses 15, (1974) 130-136.

23. F. Ohuchi, D.E. Clark and L.L. Hench, "Effect of Crystallization on the Auger Electron Signal Decay in a $\text{Li}_2\text{O} - 2 \text{SiO}_2$ Glass and Glass-Ceramic". *J. Am. Ceram. Soc.* 62 (1979) 500-503.
24. C.G. Pantano, D.G. Dove and G.Y. Onada, Jr. "AES Analysis of Sodium in a Corroded Bioglass Using a Low Temperature Technique", *Appl. Phys. Letters* 26 (1975) 601-602.
25. C.G. Pantano, D.B. Dove and G.Y. Onada, Jr., "AES Compositional Profiles of Mobile Ions in the Surface Region of Glass". *J. Vacuum Sci. Technol.* 13 (1976) 414-418.
26. F. Ohuchi, M. Ogino, P.H. Holloway and C.G. Pantano Jr, "Electron Beam Effects During Analysis of Glass Thin Films with Auger Electron Spectroscopy", *Surface - Interface Anal.* 2 (1980) 85-90.
27. A.K. Varshneya, A.R. Cooper and M. Cable, "Changes in Composition During Electron Microprobe Analysis of $\text{K}_2\text{O} - \text{SrO} - \text{SiO}_2$ Glass", *J. Appl. Phys.* 37 (1966) 2199.
28. M.P. Borom and R.E. Hanneman, "Local Compositional Changes in Alkali Silicate Glasses During Electron Microprobe Analysis". *J. Appl. Phys.* 38 (1967) 2406-2407.

29. P.J. Goodhew and J. E. C. Gulley, "The Determination of Alkali Metals in Glasses by Electron Probe Analysis", *Glass Tech.* 15 (1974) 123-126.
30. L. F. Vassamillet and F. W. Caldwell, "Electron - Probe Microanalysis of Alkali Metals in Glasses". *J. Appl. Phys.* 40 (1969) 1637-1643.
31. J.P. Vigouroux, O Lee Deacon, C. Juret, C. Boiziau and C. Le Gressus, "Surface Processes Occuring During Breakdown of High Voltage Device" *IEEE Transaction on Electrical Insulation* (1982) (to be published) .
32. J.P. Coad, H.E. Bishop and K.C. Riviere, "Electron-Beam Assisted Adsorption on the Si (111) Surface", *Surface Sci* 21 (1970) 253-264.
33. B.A. Joyce and J.H. Neave, "Electron Beam-Adsorbate Interactions on Silicon Surfaces", *Surface Sci.* 34 (1973) 401-419.
34. B.A. Joyce, "Some Aspects of the Surface Behaviour of Silicon", *Surface Sci.*, 35 (1973) 1-7.
35. R.E. Kirby and D. Lichtman, "Electron Beam Induced Effects on Gas adsorption Utilizing Auger Electron Spectroscopy ; CO and O₂ on Si. I. Adsorption Studies", *Surface Sci.* 41 (1974) 447-466.
36. R.E. Kirby and J.W. Dieball, "Electron Beam Induced Effects on Gas Adsorption Utilizing Auger Electron Spectroscopy, CO and O₂ on Si. II. Structural Effects", *Surface Sci.* 41 (1974) 467-474.
37. M.C. Muñoz and J.L. Sacedon, "Electron Stimulated Oxidation of Silicon Surfaces". *J. Chem. Phys.* 74 (1981) 4693-4700.
38. W. Ranke and K. Jacobi, "Electron Stimulated Oxidation of Ga As Studied by Quantitative Auger Electron Spectroscopy", *Surface Sci* 47 (1975) 525-542.

39. W. Ranke, "On the Magnitude of Adsorption Enhancement by Electron Beam Excitation of Molecules in the Gas Phase". *J. Phys. D*, 11 (1978) L 87-L 90.
40. Y. Margoninski, D. Segal and R.W. Kirby, "The Interference of an Electron Beam with the Surface Reaction Between Oxygen and Germanium". *Surface Sci.* 53 (1975) 488-499.
41. M. Lichtensteiger, C. Webb and J. Lagowski "Electron Stimulated Adsorption : Surface Activation and Preferential Binding of Oxygen to Sulfur on CdS". *Surface Sci.* 97 (1980) L 375 L 379.
42. J. Verhoeven and J. Los, "The Influence of an Electron Beam on Oxidation of Polycrystalline Nickel Surfaces, Monitored by Disappearance Potential Spectroscopy (DAPS)". *Surface Sci.*, 58 (1976) 566-574.
43. J. Verhoeven and J. Los, "The Influence of an Electron Beam on the Adsorption of CO and CO₂ into a Ni (110) Surface". *Surface Sci.*, 82 (1979) 109-119.
44. P.S. Frederick and S.T. Hruska", AES Study of Nickel Carburization : Electron Beam Induced Effects". *Surface Sci.*, 62 (1977) 707-719.
45. M.G. Tompkins, "The Surface Stimulated Interaction of H₂O with a Nickel Surface", *Surface Sci.* 62 (1977) 293-302.
46. P.A. Redhead, J.P. Hobson and E.V. Kornelsen in "The Physical Basis of Ultra High Vacuum". Chapman and Hill, Londres (1968), p. 167.
47. D. Menzel and R. Gomer "Desorption from Surfaces by Slow-Electron Impact". *J. Chem. Phys.* 40 (1964) 1164-1165.
48. D. Menzel and R. Gomer, "Desorption from Metal Surfaces by Low-Energy Electrons", *J. Chem. Phys.*, 41 (1964) 3311-3328.

49. P.A. Redhead, "Interaction of Slow Electrons with Chemisorbed Oxygen", *Can. J. Phys.*, 42 (1964) 886-905.
50. P.A. Redhead, "Desorption of CO and O⁺ from Polycrystalline Mo Surfaces". *Appl. Phys. Letters*, 4 (1964) 166-167.
51. P.A. Redhead, "The Effects of Adsorbed Oxygen on Measurements with Ionization Gauges", *Vacuum*, 13 (1963) 253-258.
52. P.A. Redhead, "Electron-Impact Desorption of Carbon Monoxide from Tungsten", *Suppl. Al Nuovo Cimento V*, 2 (1967), 586-597.
53. I.E. Madey and J.T. Yates, Jr., "Electron-Stimulated Desorption as a Tool for Studies of Chemisorption Review". *J. Vacuum. Sci. Technol.*, 8 n° 4 (1971) 525-554.
54. T.E. Madey and J.T. Yates, Jr, "Desorption by Electron-Impact : Oxygen Adsorbed on Tungsten", *Surface Sci.*, 11 (1968) 327-351.
55. D. Menzel, "Electron Stimulated Desorption : Principles and Recent Developments", *Surface Sci.*, 47 (1975) 370-383.
56. R. Gomer, "Chemisorption on Metals". *Sol. St. Phys.*, 30 (1975) 93-226. p. 85
57. G.E. Moore, "Dissociation of Adsorbed CO by Slow Electrons", *J. Appl. Phys.*, 32 (1961), 1241.
58. L.A. Petermann, "Gas Desorption Efficiency under Electron Bombardment (2nd. Inter. Symp. on Residual Gases in Electron Tubes, Milan, Itali (1963)).

59. H. Poppa and A. Grant-Elliott, "The Surface Composition of Mica Substrates", *Surface Sci.*, 24 (1971) 149-163.
60. C. Le Gressus, D. Massignon and R. Sopizet, "Low Beam Current Density Auger Spectroscopy and Surface Analysis". *Surface Sci.*, 68 (1977) 338-345.
61. J.S. Johannessen, W.E. Spicer and Y.E. Strausser, "An Auger Analysis of the SiO_2 -Si Interface", *J. Appl. Phys.*, 47 (1976) 3028-3037.
62. S. Ichimura and R. Shimizu, "Observation of Electron Beam Damage in Thin Film SiO_2 on Si with Scanning Auger Electron Microscope". *J. Appl. Phys.*, 50 (1979) 6020-6022.
63. A. Van Oostrom, "Some Aspects of Auger Microanalysis". *Surface Sci.* 89 (1979) 615-634.
64. T. Smith, "Auger Electron Spectroscopy and Ion Sputter Profiles of Oxides on Aluminum". *Surface Sci.* 55 (1976) 601-624.
65. L. Fiermans and J. Vennick, "Auger Electron Emission Spectroscopy of the V_2O_5 (010) and V (100) Surfaces". *Surface Sci.* 24 (1971) 541-554.
66. L. Fiermans and J. Vennick, "Inelastic Effects and Structure in the Auger Electron Emission Spectra of the V_2O_5 (010) and V (100) Surfaces : Study of Chemical Shifts". *Surface Sci.* 35 (1973) 42-62.
67. T.T. Lin and D. Lichtman, "AES Studies of Chemical Shift and Beam Effect on Molybdenum Oxides". *J. Vacuum Sci. Technol.* 15 (1978) 1689-1694.

68. T.T. Lin and D. Lichtman, "Electron Irradiation Effects on Oxidized Nb Foil and NbO". J. Mater Sci. 14 (1979) 455-461.
69. T.T. Lin and D. Lichtman, "The Effects of Electron Bombardment on the Surface Composition of WO₃, Oxidized W and Ta Foils". J. Appl. Phys. 50 (1979) 1298-1303.
70. Y. Shapira, "Electron Beam Induced Dissociation and Conductivity of SnO₂ Films". J. Appl. Phys. 52 (1981) 5696-5698.
71. M.K. Knotek and Peter J. Feibelman, "Ion Desorption by Core-Hole Auger Decay". Phys. Rev. Letters 40 (1978) 964-967.
72. Peter J. Feibelman and M.L. Knotek, "Reinterpretation of Electron Stimulated Desorption Data from Chemisorption Systems". Phys. Rev. B. 18 (1978) 6531-6539.
73. M.L. Knotek and Peter J. Feibelman, "Stability of Ionically Bonded Surfaces in Ionizing Environments". Surface Sci. 90 (1979) 78-90.
74. P.W. Palmberg and T.N. Rhodin, "Surface Dissociation of Potassium Chloride by Low Energy Electron Bombardment". J. Phys. Chem. Solids 29, (1968), 1917-1924.
75. P.D. Townsend and J.C. Kelly, "Slow Electron Induced Defects in Alkali Halides", Phys. Letters, 26 A (1968) 138-139.
76. T.E. Gallon, I.G. Higginbotham, M. Prutton and M. Tokutaka, "The Growth of Ag on KCl Observed by LEED and Auger Emission Spectroscopy". Thin Solid Films, 2 (1968), 369-373.

77. T.E. Gallon, I.G. Higginbotham, M. Prutton and M. Tolutaka, "The (100) Surfaces of Alkali Halides : I. The Air and Vacuum Cleaved Surfaces. Surface Sci., 21 (1970), 224-232.
78. M. Tolutaka, M. Prutton, I.G. Higginbotham and T.E. Gallon, "The (100) Surfaces of Alkali Halides : II. Electron Stimulated Dissociation. Surface Sci., 21 (1970), 233-240.
79. I.G. Higginbotham, T.E. Gallon, M. Prutton and M. Tokutaka, "The (100) Surfaces of Alkali Halides : III. Electron Stimulated Desorption and Overall Discussion". Surface Sci., 21 (1970) 241-252.
80. J. Durup and R.L. Platzman, "Role of the Auger Effect in the Displacement of Atoms in Solids by Ionizing Radiation". Disc. Farad. Soc., 31 (1961), 156.
81. T.R. Pian, N. Tolk, J. Kraus, M.M. Traum, J. Tully, and W.E. Collins "Electron Stimulated Desorption of Alkali Atoms from Alkali Halides Surfaces" J. Vac. Sci. Technol. 20 (1982) 555-558.
82. J.H.O. Varley, "A Mechanism for the Displacement of Ions in an Ionic Lattice", Nature, 174 (1954) 886-887.
83. J.H.O. Varley, "Discussion of Some Mechanisms of F. Centre Formation in Alkali Halides". J. Phys. Chem. Solids, 23, (1962), 985-1005.
84. T.E. Madey, C.D. Wagner and A. Joshi, "Surface Characterization of Catalysts Using Electron Spectroscopies : Results of a Round - Robin Sponsored by ASTM Committee D-32 on Catalysts". J. Electron. Spect. Relat. Phenom. 10 (1977) 359-388.

85. C.G. Pantano and T.E. Madey, "Electron Beam Damage in Auger Electron Spectroscopy". *Application of Surface Sci.* 7 (1981) 115-141.
86. J.M. Fontaine, J.P. Duraud and C. Le Gressus, "Electron Beam Effects in Auger Electron Spectroscopy and Scanning Electron Microscopy". *Surface and Interface Anal.* 1, (1979) 196-203.
87. C. Le Gressus, H. Okuzumi, D. Massignon in : *Scanning Electron Microscopy (SEM) 1981*. Ed. O. Johari (SEM. Inc., AMF O' Hare, IL, 1982). 251-261.
88. F. Pellerin, C. Le Gressus and D. Massignon, "A Secondary Electron Spectroscopy and Electron Energy Loss Spectroscopy Study of the Interaction of Oxygen with a Polycrystalline Aluminum Surface". *Surface Sci.* 103 (1981) 510-523.
89. B.H. Nall, A.N. Jette and C.B. Bargeron, "Electron Energy Loss Spectroscopy of a (111) Oriented Aluminum Single Crystal". *Surface Sci.* 110 (1981) L 606 - L 610.
90. K.L.I. Kobayashi, Y. Shiraki and Y. Katayama, "Study of Adsorption Phenomena on Aluminum by Interatomic Auger Transition Spectroscopy". *Surface Sci.* 77 (1978) 449-457.
91. P.H. Citrin, J.E. Rowe and S.B. Christman, "Interatomic Auger Transitions in Ionic Compounds". *Phys. Rev. B* 14 (1976) 2642-2658.

92. C.J. Powell and J.B. Swan, "Origin of the Characteristic Electron Energy Losses in Aluminum". Phys. Rev. 115 (1959) 869-875.
93. K.Y. Yu, J.N. Miller, P. Chye, W.E. Spicer, N.D. Lang and A.R. Williams "Study of Sorption of Oxygen on Al". Phys. Rev. B.14 (1976) 1446-1449.
94. R.Z. Bachrach, S.A. Foldström, R.S. Bauer, S.B.M. Haström and D.J. Chadi, "Surface Resonances and the Oxidation of Single-Crystal aluminum". J. Vac. Sci. Technol. 15 (2) (1978) 488-493.
95. J. Stöhr, L.I. Johansson, S. Brennan, M. Hetch and J.N. Miller, "Surface Extended-X-Ray-Absorption Fine Structure Study of Oxygen, Interaction with Al (111) Surfaces". Phys. Rev. B 22 (1980) 4052-4065.
96. R.P. Messmer, D.R. Salahub, "Chemisorption of Oxygen Atoms on Aluminum (100) : A Molecular-Orbital cluster study". Phys. Rev. B.16 (1977) 3415-3427.
97. D.R. Salahub, M. Roche and R.P. Messmer, "Chemisorption of Oxygen Atoms on Aluminum (111) : A Molecular-Orbital Cluster Study". Phys. Rev. B. 18 (1978) 6495-6505.
98. S.A. Foldström, C.W.B. Martinson, R.Z. Bachrach, S.B.M. Hagström and R.S. Bauer, "Ordered Oxygen Overlayer Associated with Chemisorption State on Al (111)", Phys. Rev. Letters 40 (1978) 907-910.

99. A.M. Bradshaw, P. Hofmann and W. Wyrobisch, "The Interaction of Oxygen with Aluminum (111)". Surface Sci. 68 (1977) 269-276.
100. J.M. Fontaine, O Lee-Deacon, J.P. Duraud, S. Ichimura and C. Le Gressus, "Electron Beam Effects on Oxygen Exposed Aluminum Surfaces". Surface Sci. 122 (1983). 40-54.
101. Y.W. Yau, R.F.W. Pease, A.A. Iranmanesh and K.J. Polansko "Generation and Applications of Finely Focussed Beams of Low Energy Electrons". J. Vac. Sci. Technol. 19 (1981), 1048-1052.

FIGURE CAPTIONS

- Figure 1 : Temperature increase versus injected power calculated on Aluminum ($K = 0,567 \text{ cal/cm.}^\circ\text{C.s}$) and on SiO_2 ($K = 32.10^{-4} \text{ cal/cm.}^\circ\text{C.s}$) for different full width (a_1) at half maximum of the electronic density of the beam.
- Figure 2 : Variation of the secondary electron emission yield δ as a function of the primary energy E_p .
- Figure 3 : Schematic representation of ESD via initial Franck-Condon transition from a bound state to a repulsive part of an ionic state. If recombination occurs at $Z > Z_c$, X can desorb as a neutral. Z_c (critical distance) is the distance at which kinetic energy E_c gained by X^+ during desorption is sufficient to overcome the potential barrier to desorb as a neutral X after recombination.
- Figure 4 : Evolution of the AES spectrum of an oxygen exposed (1000 L) Al (111) surface under electron bombardment
- 1, 2, 3 : $E_p = 230 \text{ eV} - 10^{-8} \text{ A} - 300 \text{ s}$
 4, 5 : $E_p = 5 \text{ keV} - 10^{-8} \text{ A} - 300 \text{ s}$
 6, 7, 8 : $E_p = 230 \text{ eV} - 10^{-8} \text{ A} - 300 \text{ s}.$

Figure 5 : a : Secondary electron image of the Al (111) surface after oxygen exposure (1000 L). $E_p = 230$ eV.

b : Secondary electron image of the same surface after electron bombardment ($E_p = 230$ eV ; $3,6 \times 10^{-6}$ A.cm⁻², 300 s)

The bombardment area appears with a dark contrast.

c : Secondary electron image of the same surface after electron bombardment ($E_p = 5$ keV - $3,6 \cdot 10^{-6}$ A.cm⁻², 300 s)

Secondary electron images have been done with the same primary energy : $E_p = 230$ eV.

Figure 6 : Evolution of the $E \cdot dN(E)/dE$ Auger spectrum of the Al (111) with the oxygen exposure (0 → 1000 L).

Figure 7 : Variation of the Al_{LVV} (68 eV) peak height as a function of oxygen exposure (0 → 50 L). The peak height is normalized to that recorded on a clean surface.

Figure 8 : Variations of Al_{LVV} peaks (located at 54 and 68 eV) of O_{KLL} peak (508 eV), of the sum S of the heights of the Al_{LVV} (68 eV) and Al_{LVV} (54 eV) peaks and of the ratio R (height of the Al_{LVV} (54 eV) peak on the sum S).

Figure 9 a : Variation of the O_{KLL} peak height on Al (111)

solid line : on the bombarded area (spot A)

dashed line : on the non-bombarded surface (spots B.C.D and E)

($E_p = 5 \text{ keV}$, $d = 9 \times 10^{-5} \text{ A.cm}^{-2}$).

Figure 9 b : Variation of the ratio R on Al (111)

solid line : on the bombarded area (spot A)

dashed line : on the non-bombarded surface (spots B.C.D and E)

($E_p = 5 \text{ keV}$, $d = 9 \times 10^{-5} \text{ A.cm}^{-2}$).

Figure 10 : Variation of the ratio R on Al (111) studied with two current densities

Fig. 10 a : $d = 9 \times 10^{-5} \text{ A.cm}^{-2}$

Fig. 10 b : $d = 2,3 \times 10^{-3} \text{ A.cm}^{-2}$

The initial value of R (non bombarded surface - dashed lines) is higher with $2,3 \times 10^{-3} \text{ A.cm}^{-2}$ (0,62 instead of 0,52 with $d = 9 \times 10^{-5} \text{ A.cm}^{-2}$)

Figure 11 a : Variation of the O_{KLL} peak height on Al (100)

solid line : on the bombarded area (spot A)

dashed line : on the non-bombarded surface (spots B.C.D and E)

($E_p = 5 \text{ keV}$ - $d = 9 \times 10^{-5} \text{ A.cm}^{-2}$).

Figure 11 b : Variation of the ratio R on Al (100)

solid line : on the bombarded area (spot A)

dashed line : on the non-bombarded surface (spot B.C.D and E)

($E_p = 5 \text{ keV} - d = 9 \times 10^{-5} \text{ A.cm}^{-2}$).

Figure 12 : Schematic representation of the mechanism leading to low energy electron bombardment of the sample surface.

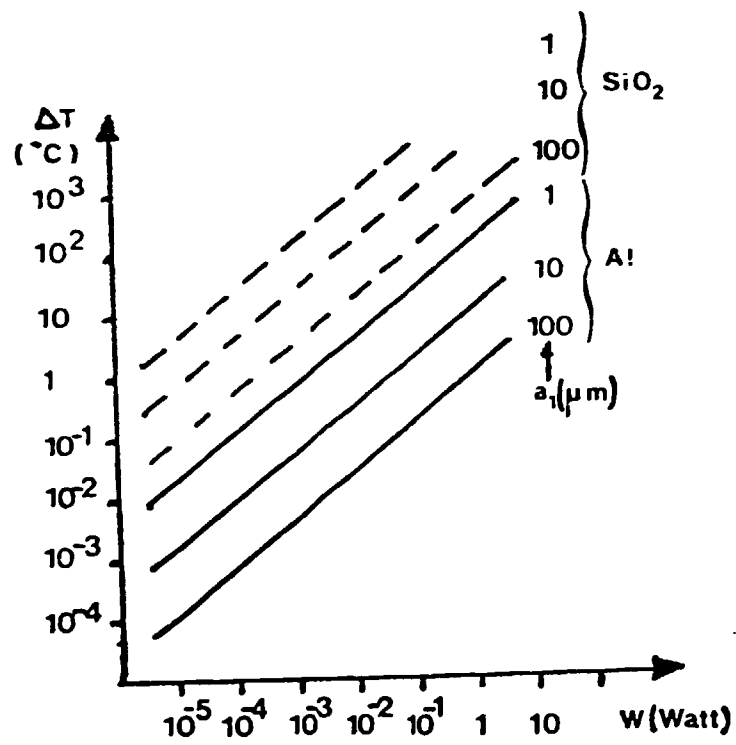


Figure 1

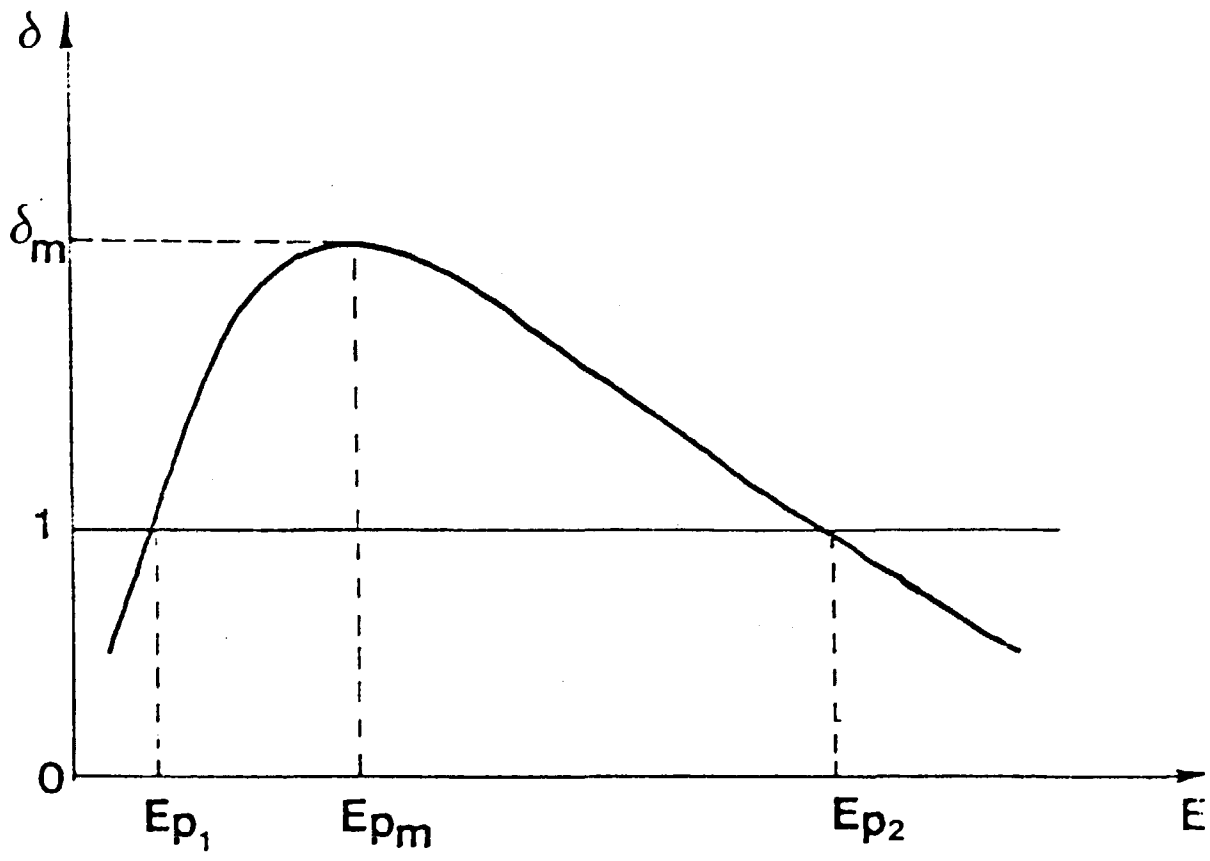


Figure 2

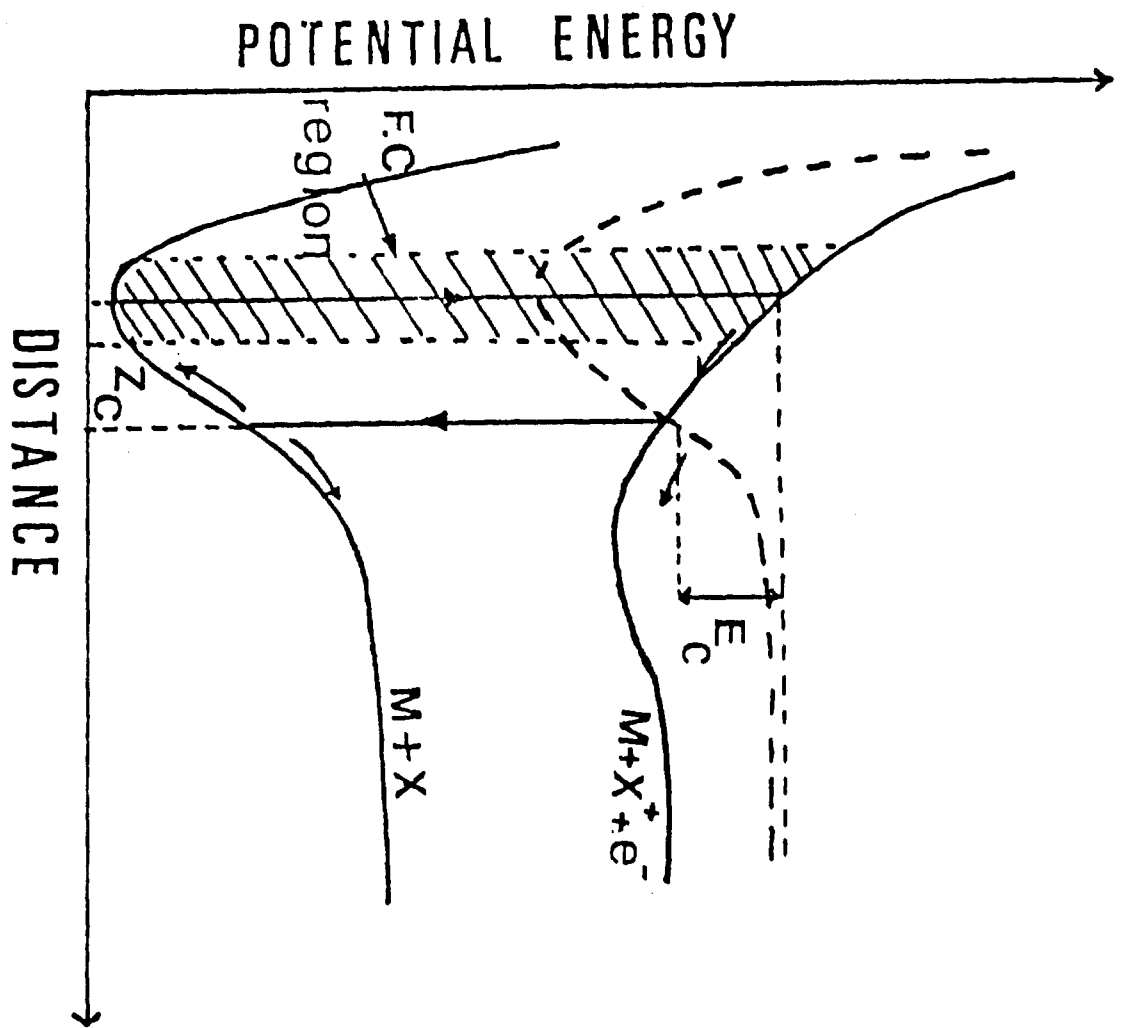


Figure 3

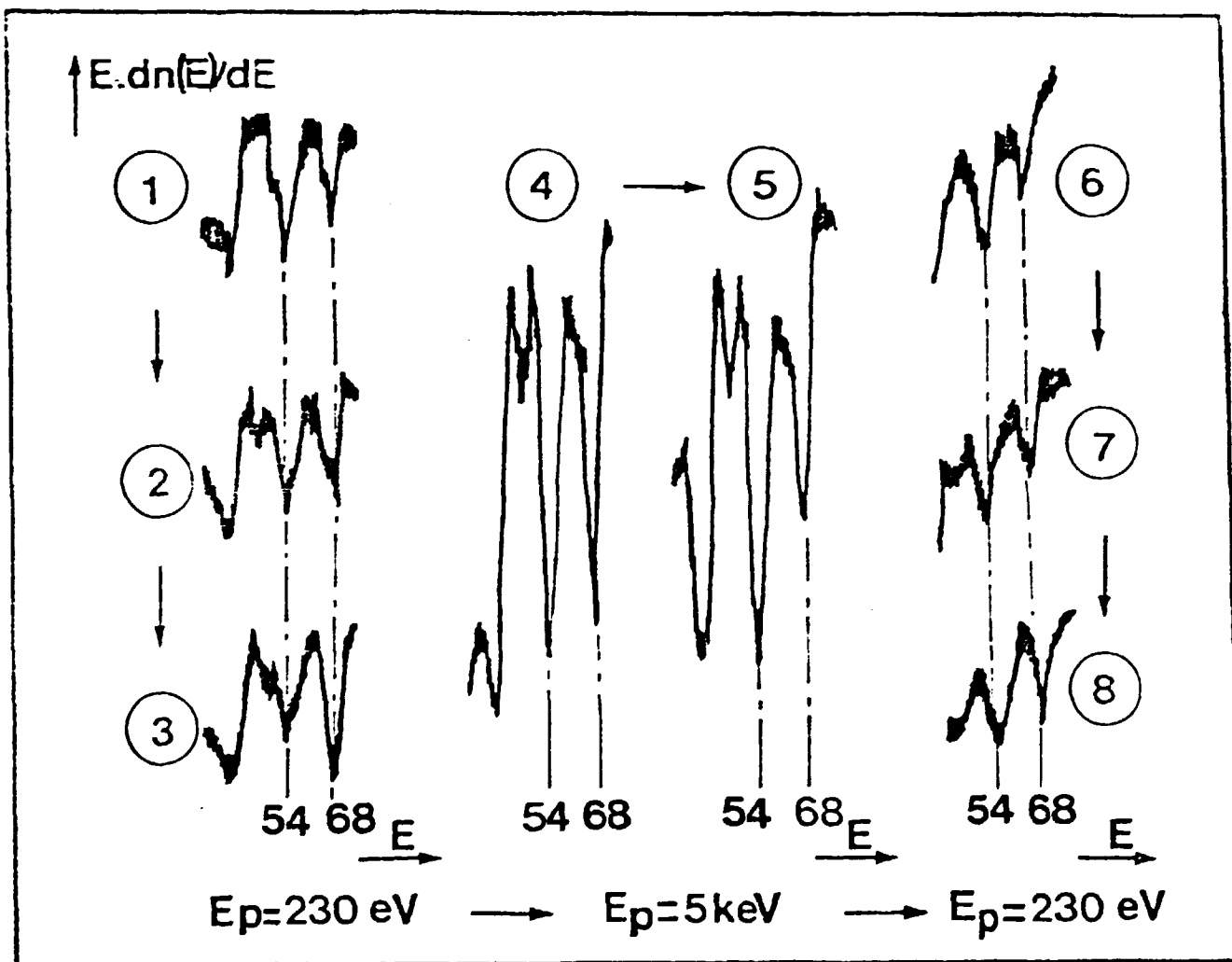
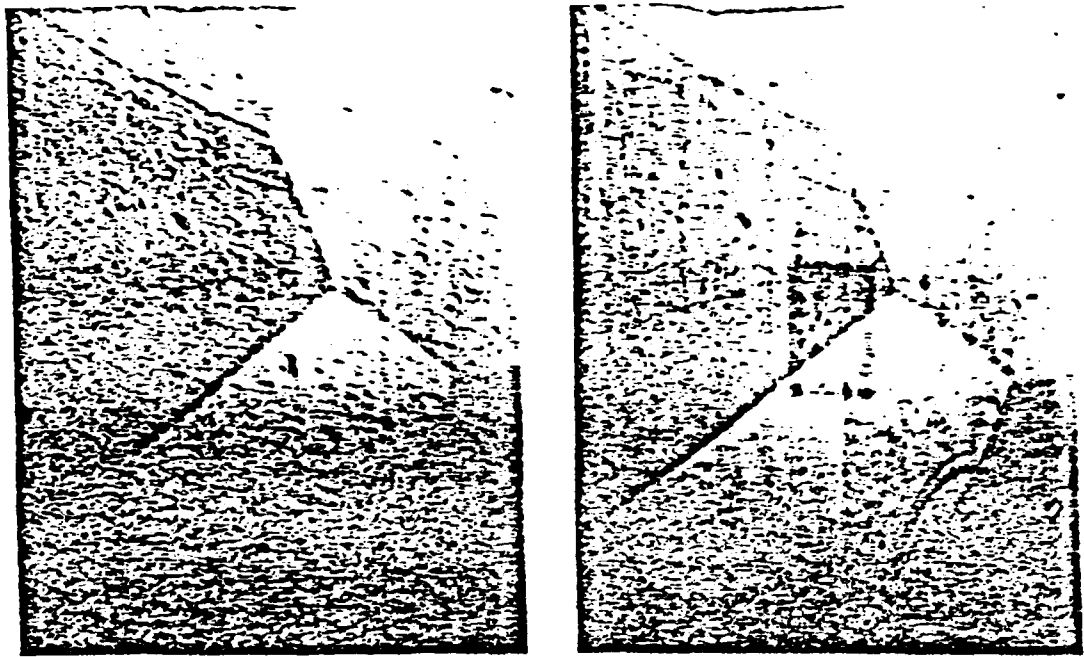


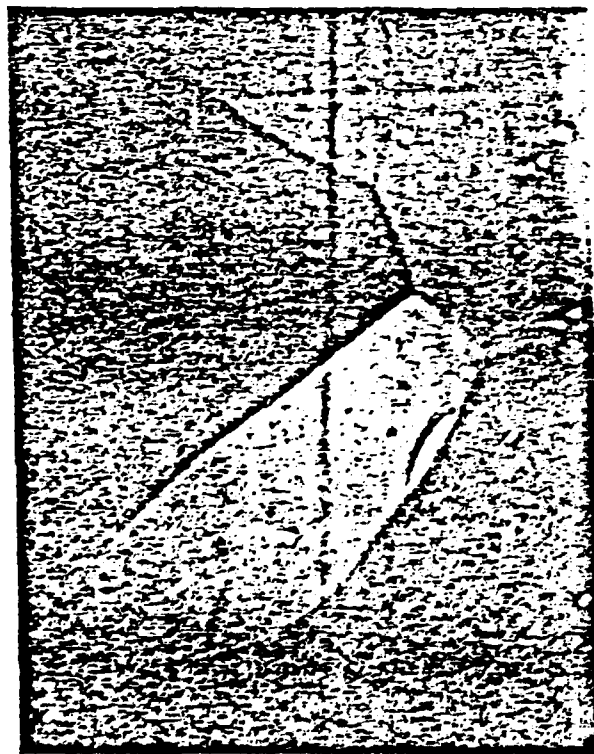
Figure 4



a

300 μm

b



c

500 μm

Figure 5

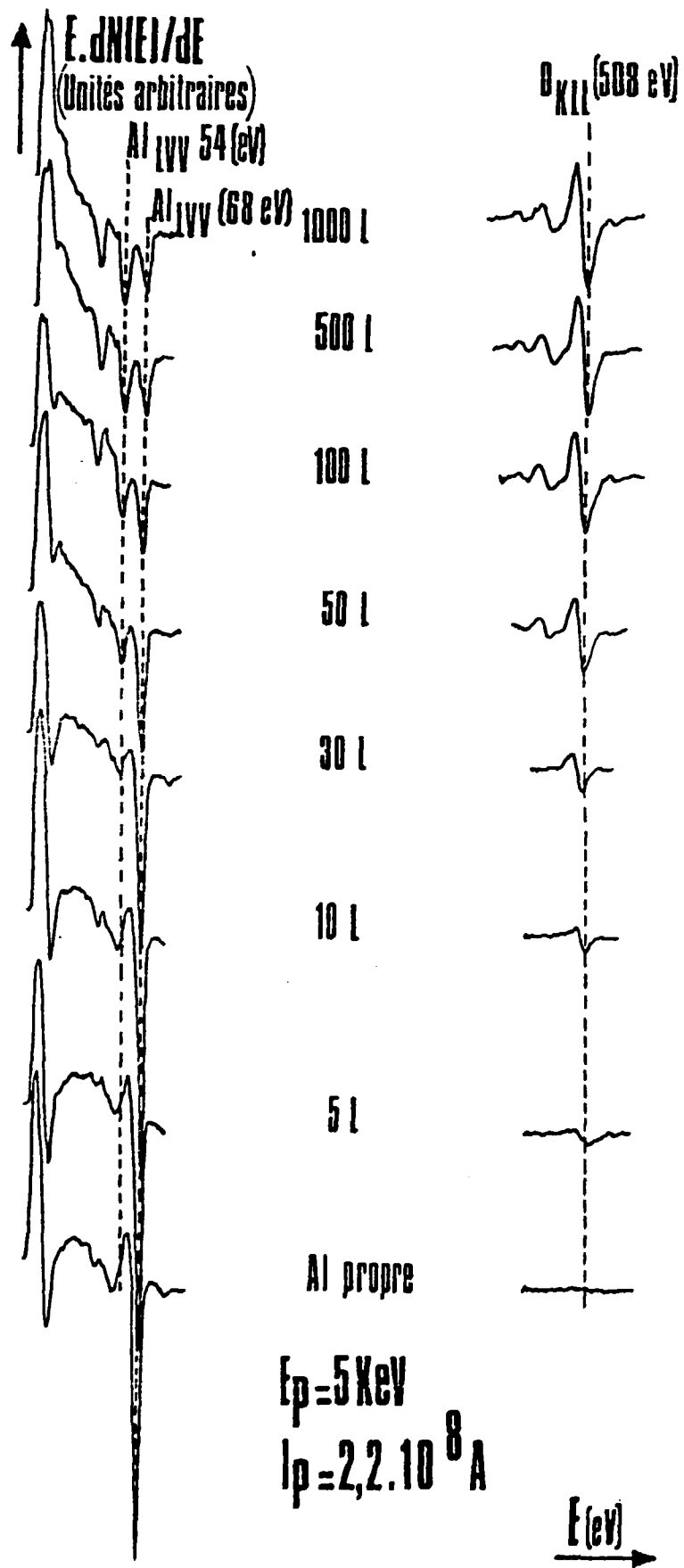


Figure 6

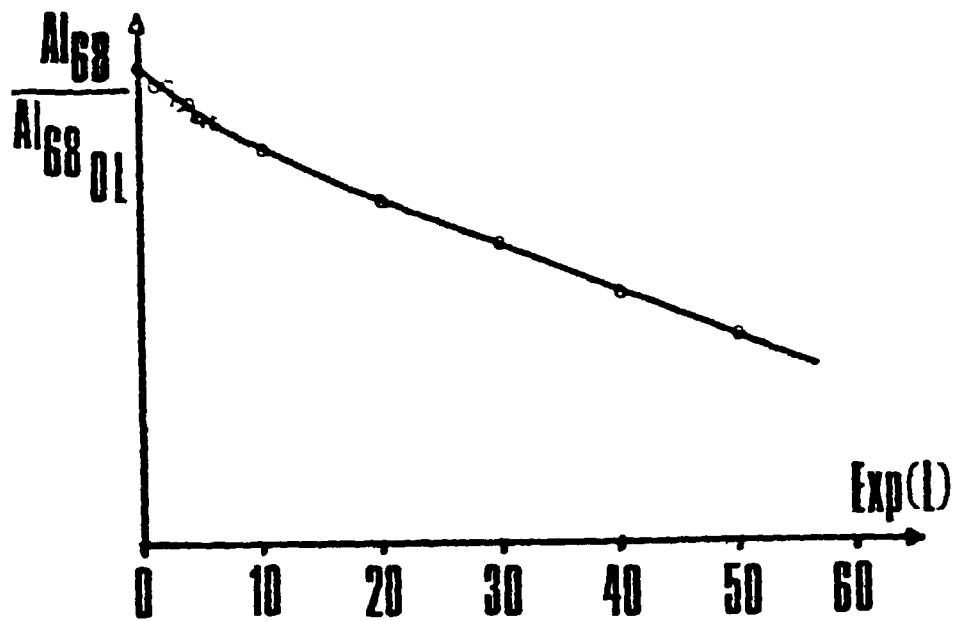


Figure 7

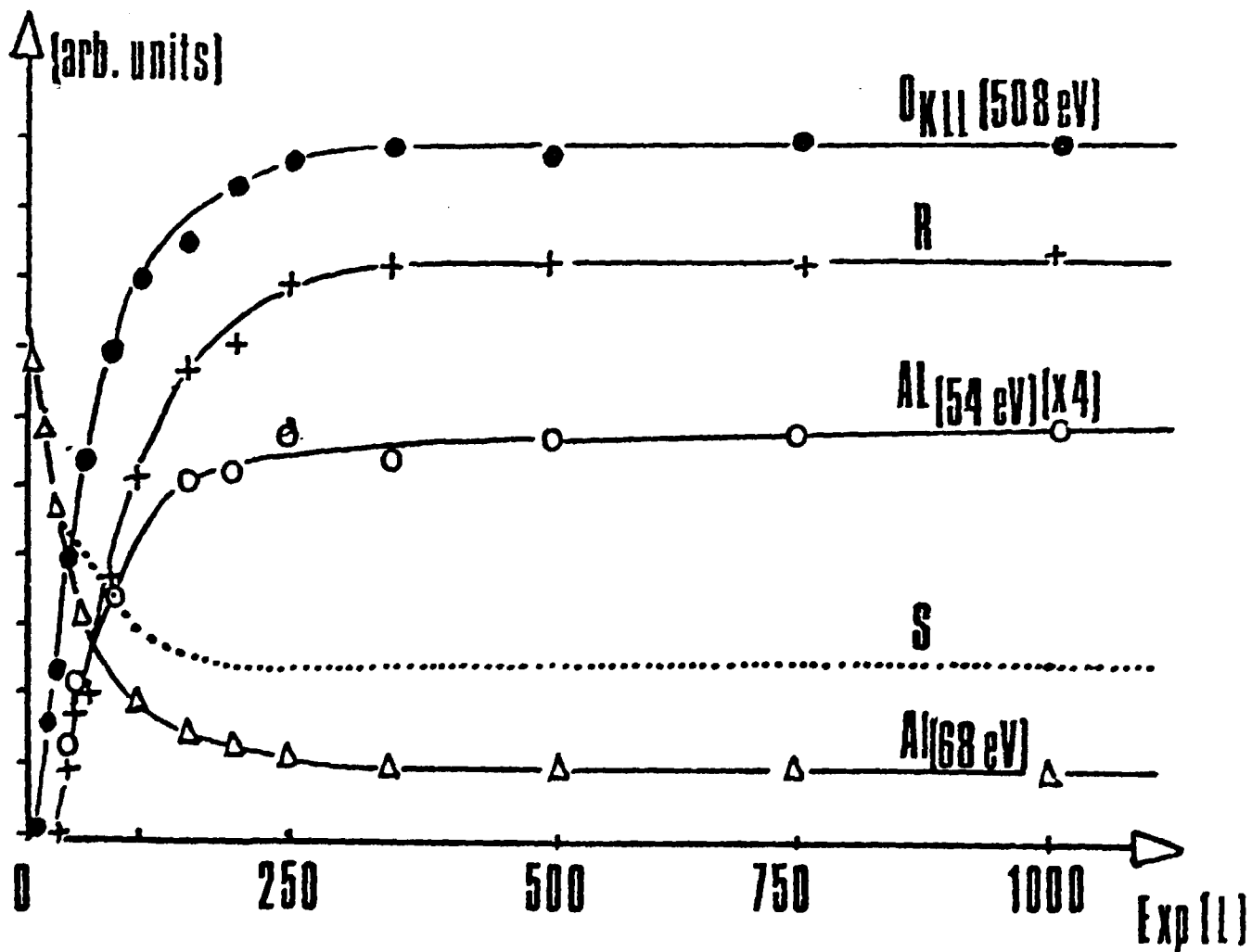


Figure 8

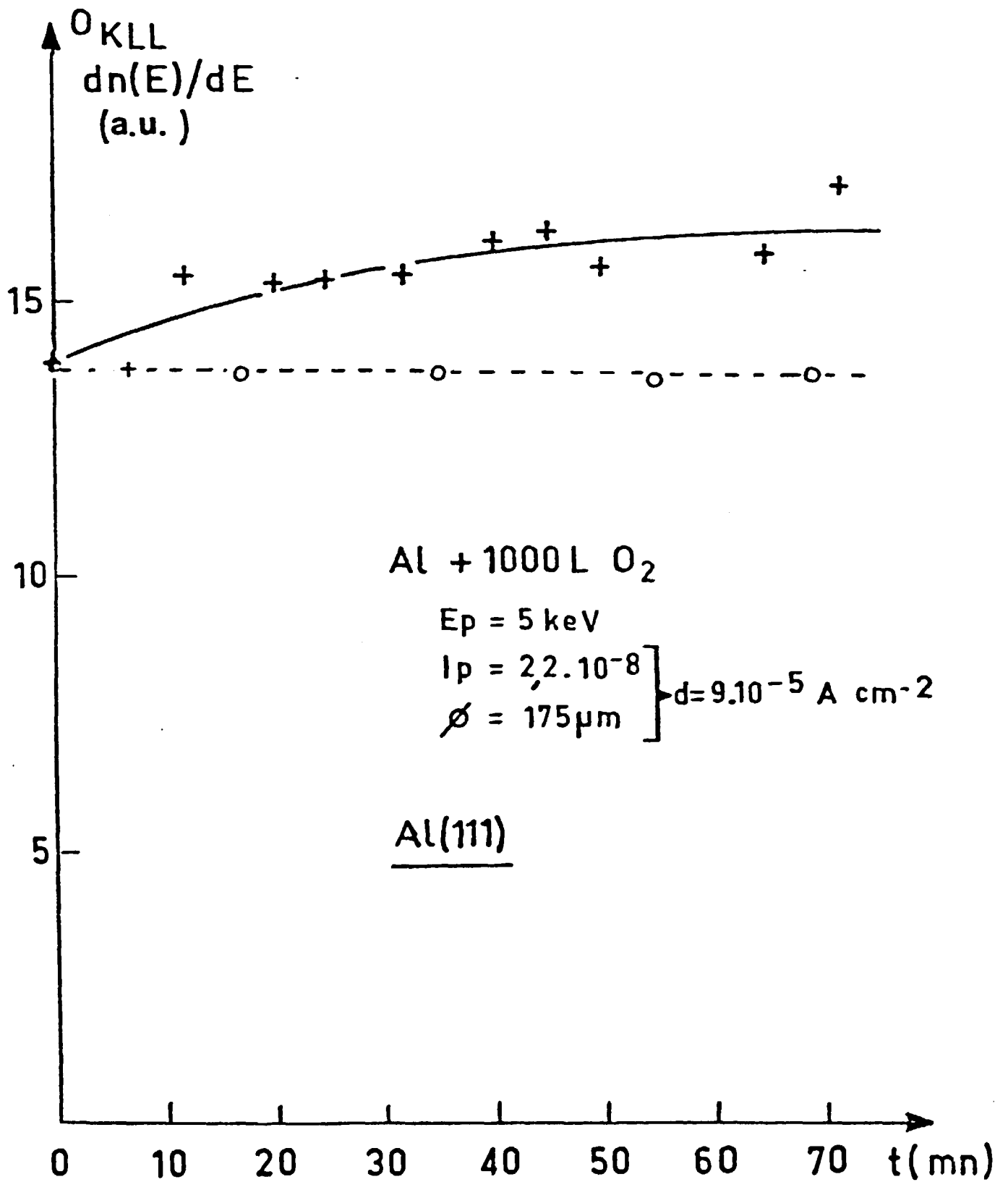
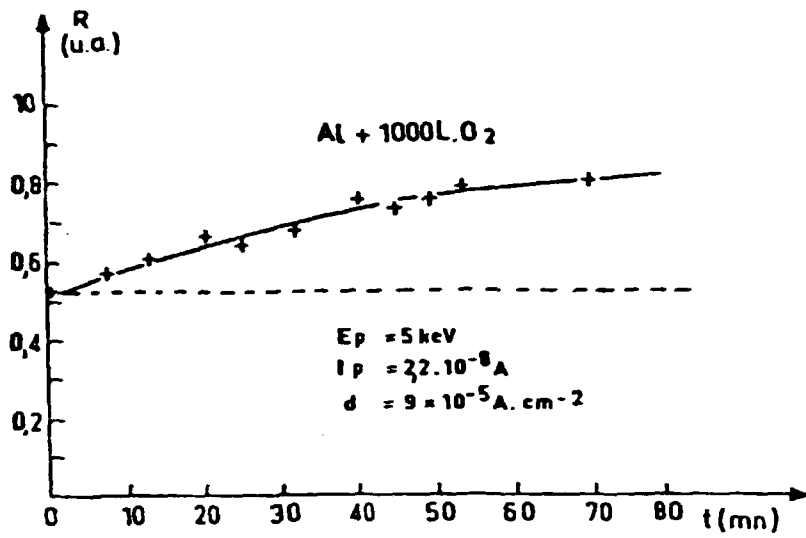
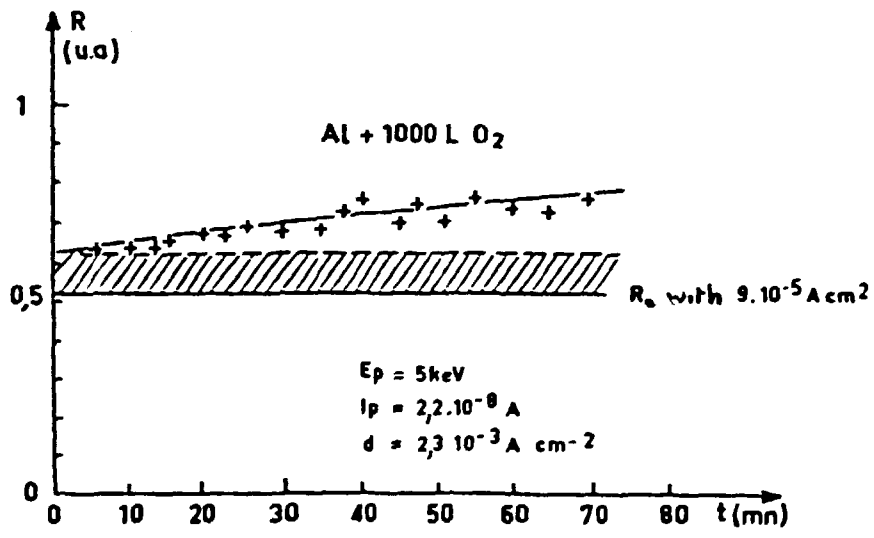


Figure 9 a

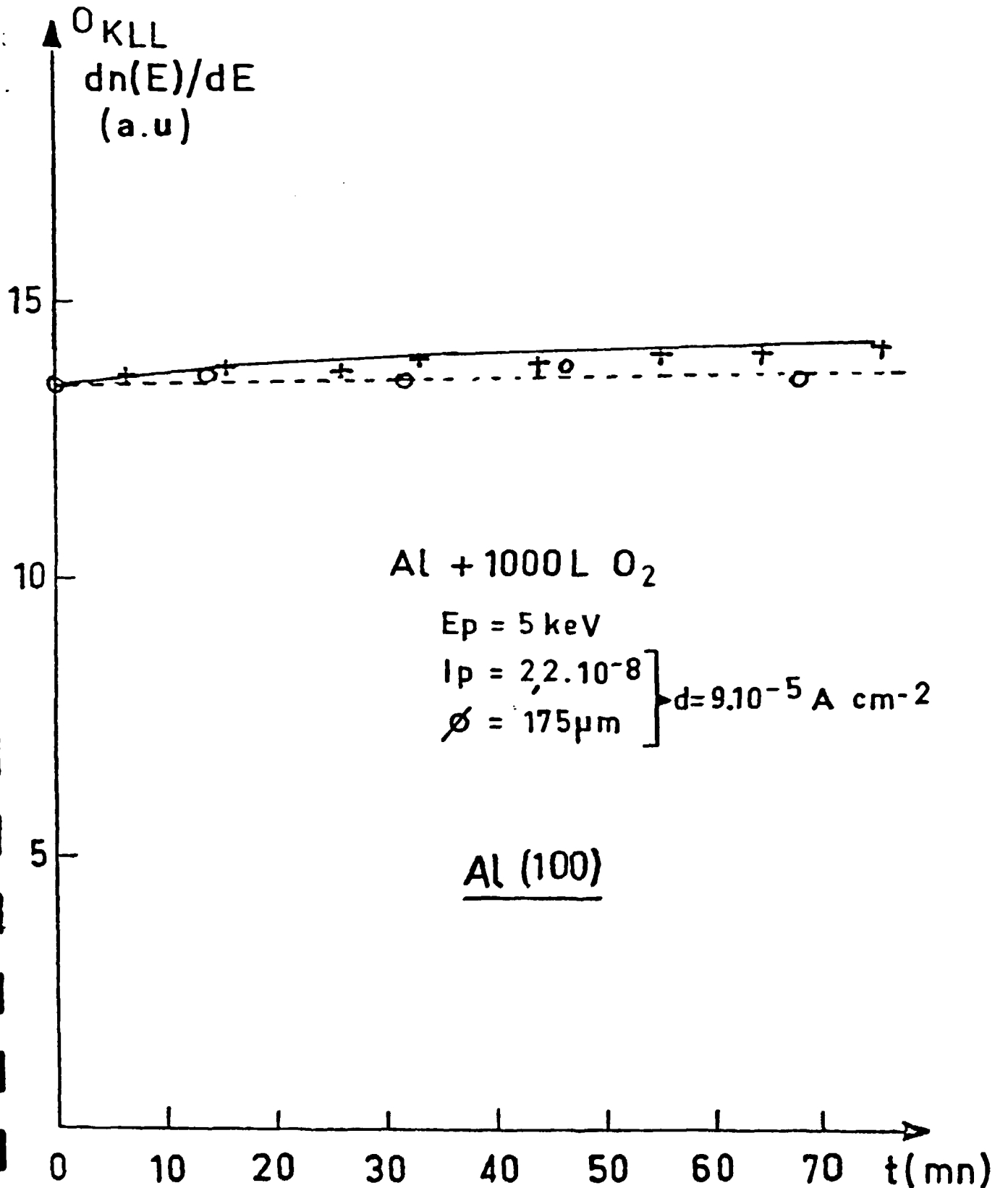


a



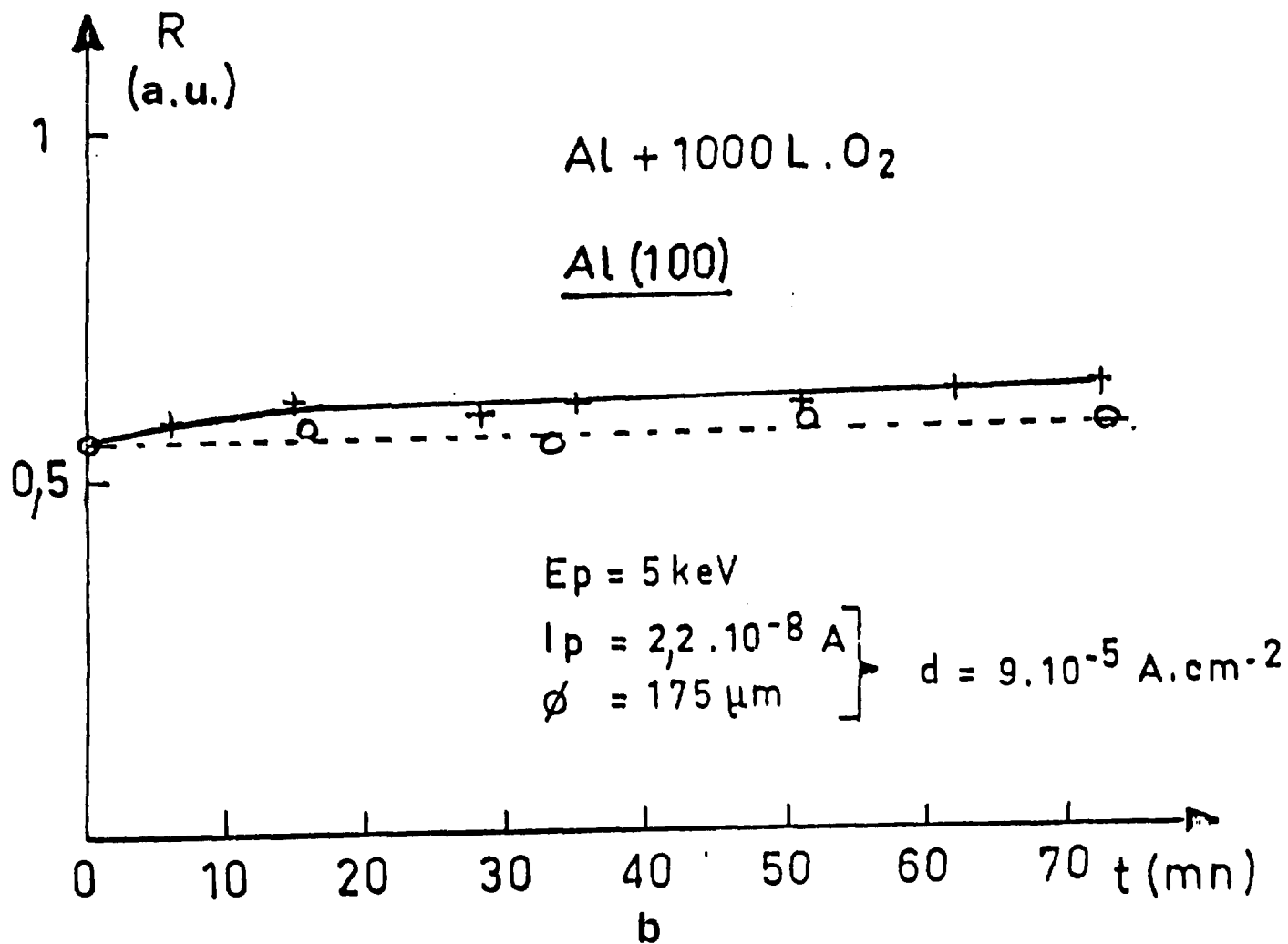
b

Figure 10



a

Figure 11 a



Figure_11_b

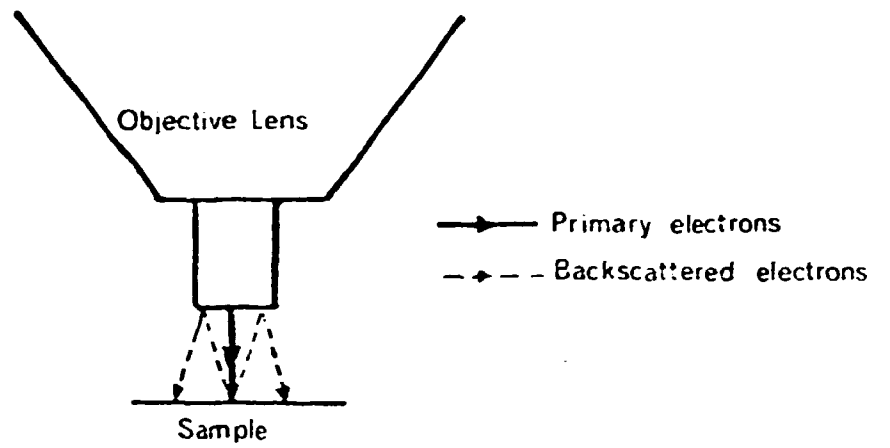


Figure 12